Physica Scripta. Vol. 56, 240–244, 1997

Relativistic Empirical Specification of Transition Probabilities from Measured Lifetime and Energy Level Data

L. J. Curtis, D. G. Ellis, R. Matulioniene and T. Brage*

Department of Physics and Astronomy, University of Toledo, Toledo, Ohio 43606, USA

Received December 28, 1996; accepted January 20, 1997

Abstract

A relativistic extension is made of methods by which intermediate coupling amplitudes are deduced from measured energy levels and combined with measured lifetimes to obtain transition probabilities within a multiplet between two pure configurations. A procedure for incorporating the relativistic j-dependence of the radial transition integral into the empirical data reduction is presented and applied to the isoelectronic formulation of the $2s^2$–$2s2p$ transitions in the Be sequence and the $6s^26p^2$–$6s^26p7s$ transitions in the Pb sequence.

1. Introduction

The multiplet of transitions that connect two configurations can be characterized, in the absence of configuration interaction (CI) effects, by a set of intermediate coupling (IC) amplitudes. In the nonrelativistic approximation, these amplitudes can be used to specify the energy level separations, relative line strengths, and magnetic g-factors of the system. Empirical methods have been developed (e.g. [1–15]) whereby the IC amplitudes are deduced from measured spectroscopic energy separations, used to predict relative line strengths and branching ratios, and combined with measured lifetimes to yield transition probability rates. The basis of these methods is the nonrelativistic Schrödinger formulation, in which the radial electric dipole (E1) transition integral has a single multiplet value. This is an overall multiplicative factor, and cancels when ratios are considered. In the relativistic Dirac formulation, the radial wavefunctions and E1 transition integrals acquire a spin dependence [16] that must be incorporated into the specification of line strengths and branching ratios from IC amplitudes. We report here a relativistic extension of these methods with applications to two specific problems: the isoelectronic systematization of line strength data for the $2s^2$–$2s2p$ resonance and intercombination transitions in the Be sequence; and the empirical specification of the branching fractions and transition probability rates of the $6s^26p^2$–$6s^26p7s$ transitions in the isoelectronic ions Pb I and Bi II.

2. Calculational formulation

Formulations of empirical methods for incorporating IC amplitudes deduced from spectroscopic energy level data into the systematization and predictive parametrization of transition probabilities have been extensively discussed and applied elsewhere [1–14]. These methods are based on the nonrelativistic Schrödinger equation, using an LS-coupling angular basis set and radial wavefunctions that are independent of j. Here we reformulate these calculations using the relativistic Dirac equation, with a jj-coupling basis set and j-dependent radial wavefunctions. This yields a more general formulation involving two j-dependent radial matrix elements, and the nonrelativistic results are recovered when these two radial matrix elements are equated.

Although this formalism is quite generally applicable, the approach will be demonstrated here for the examples of the sp and p^2 configurations. These configurations provide a particularly simple case, since the singlet-triplet mixing couples no more than two levels, hence the normalized mixing amplitudes can be expressed as mixing angles. These nonrelativistic methods have also been applied to the p^3 configuration [11], for which the mixing amplitudes comprise a matrix array, and a similar relativistic extension can be made for such cases.

2.1. *Mixing angle formulation*

We denote the IC wavefunction by $\Psi_{ljl'j'J}$ and the jj basis states by $|l_j l'_{j'} J\rangle$. In order to make comparisons with results obtained in the LS basis, the mixing angle relative to the jj basis will be written as Θ_J–θ_J, where Θ_J is the jj-limit value of the mixing angle θ_J which is defined in the LS basis.

For an sp configuration there are four levels (denoted in LS notation as $^3P^o_0$, $^3P^o_1$, $^3P^o_2$, $^1P^o_1$) which can be written as

$$\Psi_{s(1/2)p(1/2)0} = |s_{1/2}\, p_{1/2}\, 0\rangle, \tag{1}$$

$$\Psi_{s(1/2)p(1/2)1} = \cos(\Theta_1 - \theta_1)|s_{1/2}\, p_{1/2}\, 1\rangle - \sin(\Theta_1 - \theta_1)|s_{1/2}\, p_{3/2}\, 1\rangle, \tag{2}$$

$$\Psi_{s(1/2)p(3/2)2} = |s_{1/2}\, p_{3/2}\, 2\rangle, \tag{3}$$

$$\Psi_{s(1/2)p(3/2)1} = \sin(\Theta_1 - \theta_1)|s_{1/2}\, p_{1/2}\, 1\rangle + \cos(\Theta_1 - \theta_1)|s_{1/2}\, p_{3/2}\, 1\rangle. \tag{4}$$

For a p^2 configuration there are five levels (denoted in LS notation as $^3P_0$, $^3P_1$, $^3P_2$, $^1D_2$, $^1S_0$) which can be written as

$$\Psi_{p(1/2)p(1/2)0} = \cos(\Theta_0 - \theta_0)|p_{1/2}\, p_{1/2}\, 0\rangle - \sin(\Theta_0 - \theta_0)|p_{3/2}\, p_{3/2}\, 0\rangle, \tag{5}$$

$$\Psi_{p(1/2)p(3/2)1} = |p_{1/2}\, p_{3/2}\, 1\rangle, \tag{6}$$

$$\Psi_{p(1/2)p(3/2)2} = \cos(\Theta_2 - \theta_2)|p_{1/2}\, p_{3/2}\, 2\rangle - \sin(\Theta_2 - \theta_2)|p_{3/2}\, p_{3/2}\, 2\rangle, \tag{7}$$

$$\Psi_{p(1/2)p(3/2)2} = \sin(\Theta_2 - \theta_2)|p_{1/2}\, p_{3/2}\, 2\rangle + \cos(\Theta_2 - \theta_2)|p_{3/2}\, p_{3/2}\, 2\rangle, \tag{8}$$

$$\Psi_{p(3/2)p(3/2)0} = \sin(\Theta_0 - \theta_0)|p_{1/2}\, p_{1/2}\, 0\rangle + \cos(\Theta_0 - \theta_0)|p_{3/2}\, p_{3/2}\, 0\rangle. \tag{9}$$

The s^2 configuration provides a convenient transition partner for the sp, and has only one level (in LS notation

* Permanent address: Fysiska Institutionen, Lunds Universitet, Lund, Sweden

$^1S_0$)

$$\Psi_{s(1/2)s(1/2)0} = |s_{1/2}\, s_{1/2}\, 0\rangle. \tag{10}$$

Since the mixed configurations contain more energy level intervals than Slater parameters, the mixing angles can be obtained from the measured spectroscopic energy values in an overdetermined manner. This overdetermination can first be removed by considering the average energy ε_J for each value of $J = 0, 1, 2, 3$, and then used to test the purity of the configuration by noting the accuracy with which that formulation reproduces the measured J-splitting.

In terms of these J-centroid energies, the mixing angles can be obtained for the sp configuration using

$$\cot(2\theta_1) = \frac{\varepsilon_2 - 3\varepsilon_1 + 2\varepsilon_0}{\sqrt{2}(\varepsilon_2 - \varepsilon_0)} \tag{11}$$

and for the p^2 configuration using

$$\cot(2\theta_0) = -\frac{10\varepsilon_2 - 21\varepsilon_1 + 11\varepsilon_0}{4\sqrt{2}(5\varepsilon_2 - 3\varepsilon_1 - 2\varepsilon_0)}, \tag{12}$$

$$\cot(2\theta_2) = -\frac{5\varepsilon_2 + 3\varepsilon_1 - 8\varepsilon_0}{2\sqrt{2}(5\varepsilon_2 - 3\varepsilon_1 - 2\varepsilon_0)}. \tag{13}$$

The one electron radial integrals will be denoted as

$$R_{11} \equiv \langle s_{1/2}|r|p_{1/2}\rangle, \tag{14}$$

$$R_{13} \equiv \langle s_{1/2}|r|p_{3/2}\rangle. \tag{15}$$

2.2. *Transitions between s^2 and sp configurations*

Using the wavefunctions from eqs (1)–(4) and eq. (10)

$$\langle \Psi_{s(1/2)s(1/2)0}\|\boldsymbol{r}\|\Psi_{s(1/2)p(1/2)1}\rangle = \frac{1}{\sqrt{3}}[R_{11}\cos(\Theta_1 - \theta_1) - \sqrt{2}R_{13}\sin(\Theta_1 - \theta_1)], \tag{16}$$

$$\langle \Psi_{s(1/2)s(1/2)0}\|\boldsymbol{r}\|\Psi_{s(1/2)p(3/2)1}\rangle = \frac{1}{\sqrt{3}}[R_{11}\sin(\Theta_1 - \theta_1) + \sqrt{2}R_{13}\cos(\Theta_1 - \theta_1)]. \tag{17}$$

Using $\tan\Theta_1 = 1/\sqrt{2}$ and trigonometric reduction formulae, these can be rewritten in the convenient form

$$\langle \Psi_{s(1/2)s(1/2)0}\|\boldsymbol{r}\|\Psi_{s(1/2)p(1/2)1}\rangle = \sqrt{\frac{R_{11}^2 + 2R_{13}^2}{3}}\sin(\theta_1 - \xi), \tag{18}$$

$$\langle \Psi_{s(1/2)s(1/2)0}\|\boldsymbol{r}\|\Psi_{s(1/2)p(3/2)1}\rangle = \sqrt{\frac{R_{11}^2 + 2R_{13}^2}{3}}\cos(\theta_1 - \xi), \tag{19}$$

where

$$\tan\xi \equiv \sqrt{2}\,\frac{R_{13} - R_{11}}{2R_{13} + R_{11}}. \tag{20}$$

Notice that in the nonrelativistic LS coupling limit where $R = R_{11} = R_{13}$, this becomes

$$\langle {}^1S_0\|\boldsymbol{r}\|{}^3P_1\rangle = R\sin\theta_1, \tag{21}$$

$$\langle {}^1S_0\|\boldsymbol{r}\|{}^1P_1\rangle = R\cos\theta_1 \tag{22}$$

which is the form that was used in empirical formulation of Refs [1, 3].

2.3. *Transitions between p^2 and sp configurations*

For the p^2 – sp manifold many transitions are possible. For brevity, we shall restrict consideration to those involving $\Psi_{s(1/2)p(1/2)1}$, which occurs in the application treated below. (For the Pb-like $6p^2$–$6p7s$ transitions, the upper level $^3P_1^o$ is chosen because the $^3P_0^o$ is unbranched whereas the $^3P_2^o$ and $^1P_1^o$ have branches to other configurations.) Using the wavefunctions of eqs (5)–(9) and eq. (2), substituting $\tan\Theta_0 = \cot\Theta_2 = 1/\sqrt{2}$ and using trigonometric reduction formula, these integrals become

$$\langle \Psi_{p(1/2)p(1/2)0}\|\boldsymbol{r}\|\Phi_{s(1/2)p(1/2)1}\rangle = -\frac{\sqrt{20}}{3}[(R_{13} + 2R_{11})\cos\theta_0\cos\theta_1 - (2R_{13} + R_{11})\sin\theta_0\sin\theta_1 + \sqrt{2}(R_{13} - R_{11})\sin(\theta_0 - \theta_1)], \tag{23}$$

$$\langle \Psi_{p(1/2)p(1/2)1}\|\boldsymbol{r}\|\Psi_{s(1/2)p(1/2)1}\rangle = \frac{\sqrt{15}}{3}[(2R_{13} + R_{11})\cos\theta_1 + \sqrt{2}(R_{13} - R_{11})\sin\theta_1], \tag{24}$$

$$\langle \Psi_{p(1/2)p(3/2)2}\|\boldsymbol{r}\|\Psi_{s(1/2)p(1/2)1}\rangle = \tfrac{5}{3}[(4R_{13} + 2R_{11})\sin\theta_1\sin\theta_2 + (4R_{13} - R_{11})\cos\theta_1\cos\theta_2 - \sqrt{2}(R_{13} - R_{11})\sin(\theta_1 - \theta_2)], \tag{25}$$

$$\langle \Psi_{p(3/2)p(3/2)2}\|\boldsymbol{r}\|\Psi_{s(1/2)p(1/2)1}\rangle = -\tfrac{5}{3}[(4R_{13} + 2R_{11})\sin\theta_1\cos\theta_2 - (4R_{13} - R_{11})\cos\theta_1\sin\theta_2 + \sqrt{2}(R_{13} - R_{11})\cos(\theta_1 - \theta_2)], \tag{26}$$

$$\langle \Psi_{p(3/2)p(3/2)0}\|\boldsymbol{r}\|\Psi_{s(1/2)p(1/2)1}\rangle = -\frac{\sqrt{20}}{3}[(R_{13} + 2R_{11})\sin\theta_0\cos\theta_1 + (2R_{13} + R_{11})\cos\theta_0\sin\theta_1 - \sqrt{2}(R_{13} - R_{11})\cos(\theta_0 - \theta_1)]. \tag{27}$$

Notice that in the nonrelativistic LS coupling limit where $R = R_{11} = R_{13}$ these become

$$\langle {}^3P_0\|\boldsymbol{r}\|{}^3P_1^o\rangle = -\sqrt{20}R\cos(\theta_0 + \theta_1), \tag{28}$$

$$\langle {}^3P_1\|\boldsymbol{r}\|{}^3P_1^o\rangle = \sqrt{15}R\cos\theta_1, \tag{29}$$

$$\langle {}^3P_2\|\boldsymbol{r}\|{}^3P_1^o\rangle = 5R[2\sin\theta_1\sin\theta_2 + \cos\theta_1\cos\theta_2], \tag{30}$$

$$\langle {}^1D_2\|\boldsymbol{r}\|{}^3P_1^o\rangle = -5R[2\sin\theta_1\cos\theta_2 - \cos\theta_1\sin\theta_2], \tag{31}$$

$$\langle {}^1S_0\|\boldsymbol{r}\|{}^3P_1^o\rangle = -\sqrt{20}R\sin(\theta_0 + \theta_1). \tag{32}$$

which is the form that was used in the empirical development of Ref. [4].

2.4. *Line strengths and branching ratios*

The matrix elements can then be used to specify the line strength factor S_{ik}

$$S_{ik} = |\langle \Psi_i|\boldsymbol{r}|\Psi_k\rangle|^2. \tag{33}$$

This can then be used to specify the transition probability rates A_{ik}

$$g_i A_{ik}(\mathrm{ns}^{-1}) = \left[\frac{1265.38}{\lambda(\text{Å})}\right] S_{ik} \tag{34}$$

which are related to the lifetime τ_i through the branching fractions BF_{ik} by

$$BF_{ik} = A_{ik}\tau_i. \tag{35}$$

3. Applications

In order to investigate the significance of these relativistic corrections, we have carried out calculations of the quantity R_{13}/R_{11} for a variety of systems using the multi-configuration Dirac–Fock program GRASP [17]. These results indicate that the ratio is most likely to deviate from unity in a situation where the integral is heavily affected by cancellation effects. However, even if the ratio differs only slightly from unity, the corrections can be important if the formalism is to be applied to a situation for which the singlet-triplet mixing is small, but still dominant over perturbations from mixing with other configurations.

We have therefore chosen to present one example from each of these situations. The first involves the Be isoelectronic sequence where ξ is small, but not negligible compared to θ_1. The second involves the Pb isoelectronic sequence, where the E1 transition matrix is affected by cancellation, and exhibits a value for R_{13}/R_{11} that differs substantially from unity. Both systems have been shown to be virtually free of CI.

3.1. *Line strengths for Be-like $2s^2$–$2s2p$ transitions*

It has been demonstrated that the measured line strengths of the resonance and intercombination transitions $ns^2\,{}^1S_0$–$nsnp\,{}^1P_1$ and $ns^2\,{}^1S_0$–$nsnp\,{}^3P_1$ in alkaline earthlike systems can be isoelectronically linearized by the use of eqs (21) and (22). If the measured line strengths are denoted by S(Res) and S(Int), then eqs (21) and (22) permit their exposition in the form of the reduced line strengths S_r(Res) and S_r(Int), defined as

$$S_r(\text{Res}) \equiv S(\text{Res})/\cos^2\theta_1 \tag{36}$$

$$S_r(\text{Int}) \equiv S(\text{Int})/\sin^2\theta_1. \tag{37}$$

With this reduction, the data have been observed in many cases [2–8] to conform to a linear relationship

$$Z^2 S_r = S_0 + b/(Z - C) \tag{38}$$

where C is an empirically chosen screening constant and S_0 is the corresponding hydrogenic value of the line strength.

An exposition of the data for the $2s^2$–$2s2p$ transitions in the Be sequence (taken from Ref. [3]) is shown in Fig. 1(a). Here the resonance and intercombination lines follow a linear behaviour that appears to converge to a value at high Z that corresponds to

$$S_0 = \tfrac{2}{3}(\sqrt{3}\cos\phi - \sin\phi)^2 S_H = 38.5, \tag{39}$$

where $S_H = 54$ is the 2s–2p line strength for hydrogen and $\phi = 13°$ is the asymptotic $2s^2$–$2p^2$ mixing computed [3] by diagonalizing the matrix of the Coulomb repulsion using standard Slater-integral methods and hydrogenic wavefunctions.

The absence of other significant effects of CI in this system is evidenced by the high degree of reliability with which the mixing angles predict the overdetermined levels of the system [3]. Thus the fact that the resonance and intercombination have slightly different slopes suggests that the nonrelativistic assumption of a j-independent radial matrix element should be reexamined in the context of the development presented here. If eqs (18) and (19) were instead used to define the reduced line strengths, eqs (36) and (37) would become

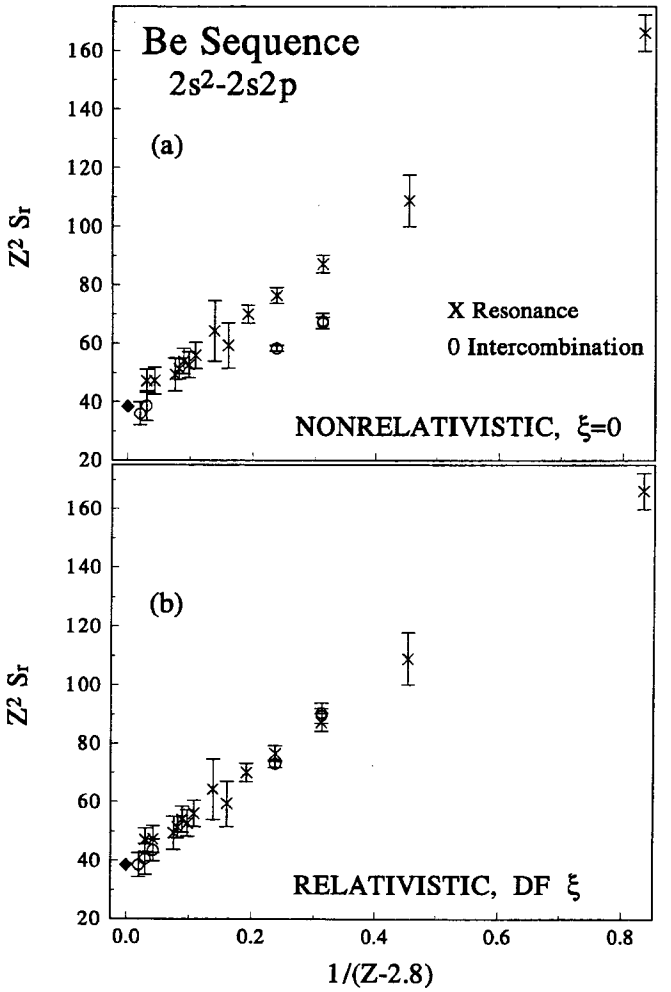

Fig. 1. Reduced line strength *vs.* reciprocal screened charge for the Be-like $2s^2$–$2s2p$ resonance and intercombination transitions with (a) nonrelativistic reduction [eqs (36) and (37)] and (b) relativistic reduction [eqs (40) and (41)].

$$S_r(\text{Res}) = S(\text{Res})/\cos^2(\theta_1 - \xi), \tag{40}$$

$$S_r(\text{Int}) = S(\text{Int})/\sin^2(\theta_1 - \xi). \tag{41}$$

To test this procedure, we have computed the ratio R_{13}/R_{11} for this system using the Dirac–Fock code [17]. The values obtained for ξ using eq. (20) are shown in Fig. 2, together with the empirical singlet–triplet mixing angle θ_1 upon which the exposition in Fig. 1(a) was based [3]. These quantities were used to produce a revised exposition of these data which is shown in Fig. 1(b). The data sources used here are the same as cited in Ref. [3]. Figure 1(b) shows that the use of these simple single configuration Dirac–Fock estimates for the R_{13}/R_{11} factors has caused the trends of the resonance and intercombination transition data to merge into a single linear trend. The fact that the resonance and intercombination data merge in this exposition suggests that measurements of one of them can be used to predict the other. Since resonance transitions tend to be very short-lived at high Z and intercombination transitions tend to be very long-lived at low Z, their common formulation is predictively useful.

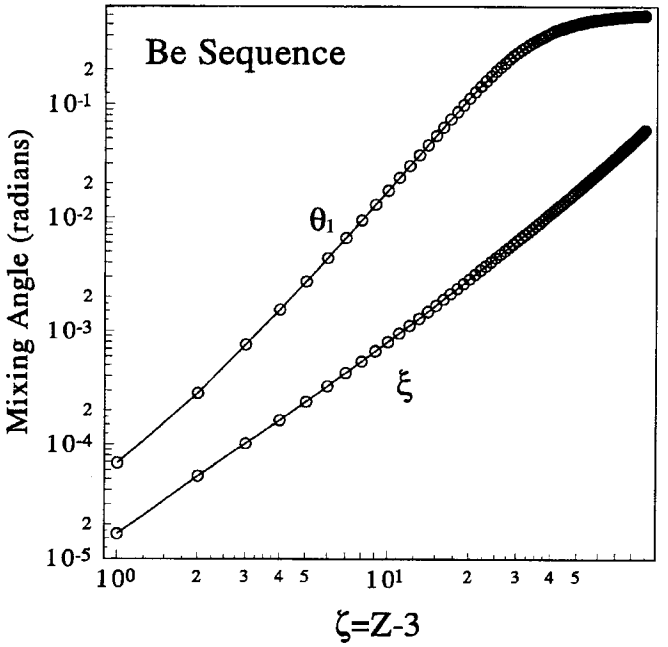

Fig. 2. Mixing angle [from eq. (11)] and relativistic radial integral factor [from eq. (20)] for the Be-like $2s^2$–2s2p transitions.

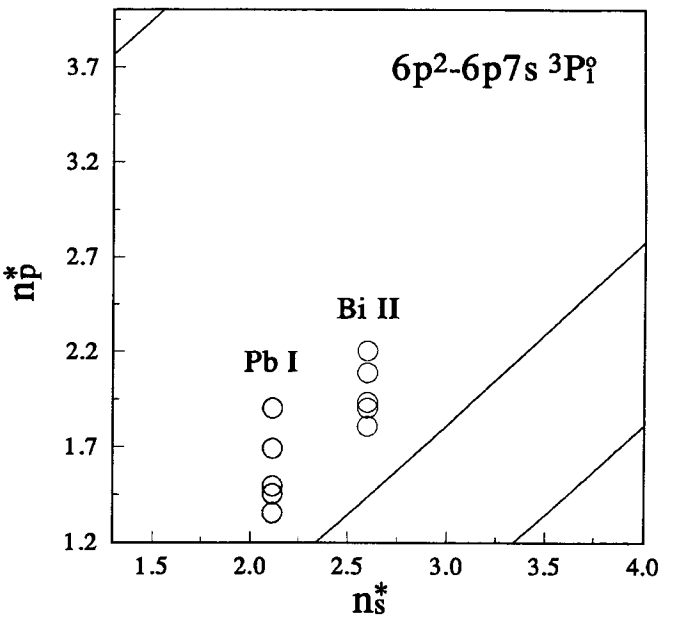

Fig. 3. Quantum defect plot for $6p^2$–6p7s transition in Pb I and Bi II. Large cancellation effects are expected when the experimental data (○) are near a predicted nodal line.

3.2. *Branching fractions for Pb-like $6s^26p^2$–$6s^26p7s$ transitions*

The $6s^26p^2$–$6s^26p7s$ transitions near the neutral end of the Pb isoelectronic sequence provide an example in which both the upper and lower configurations are relatively free of CI, but both are significantly mixed by IC. The lack of CI in these levels for Pb I is evidenced by measurements [19] of their magnetic g-factors, which are in very close agreement with IC-based predictions. Similarly, the lack of CI in these levels for Bi II is evidenced by the agreement that is obtained between the measured energy levels and the values predicted by the overdetermined mixing angles [4]. A number of studies have been published for Pb I [12] and Bi II [4, 13, 14] in which branching fractions are computed for IC mixing angles and used to deduce transition probability rates from measured lifetimes [4, 23].

The E1 transition moments in this sequence are significantly affected by cancellations in the integral. This can be seen from a cancellation exposition based on the nonrelativistic Coulomb approximation [24] which is shown in Fig. 3. In this formulation, the conditions of cancellation can be represented by nodal lines in a space constructed of the effective quantum numbers of the upper and lower states. The degree of cancellation for a physical ion can be estimated from the proximity of its effective quantum numbers to a node when exhibited on this plot. Figure 3 displays the effective quantum numbers of the transitions from the $6p^2\ ^3P_0$, $^3P_1$, $^3P_2$, $^1D_2$ and $^1S_1$ lower levels to the $6s6p\ ^3P^o_1$ upper level for Pb I and Bi II. Although the physical points do not fall directly on a node (which would imply complete cancellation) their proximity to it suggests that small differences between the j-dependent wavefunctions could lead to large differences in the integrand.

We performed Dirac–Fock [17] calculations of R_{13}/R_{11} for this sequence, obtaining the values given in Table I for Pb I and Bi II. For ions heavier than Bi II the values increased approximately as $(Z-81)^2$, reaching 1.551 at U XI. Table I also lists values for θ_2, θ_0 and θ_1 deduced from measured energy level data, as well as lifetime measurements for the $^3P^o_1$ level.

Tables II and III compare the results of nonrelativistic [eqs (23)–(27)] and relativistic [eqs (28)–(32)] calculations of the branching fractions for Pb I and Bi II. Consistent with the deviation from unity of the quantity R_{13}/R_{11}, there are significant differences between the relativistic and nonrelativistic calculations. As shown in Table II, branching fraction measurements are available for the Pb I case, and these are in much closer agreement with the relativistically computed branching fractions. For this reason we have adopted

Table I. *Empirical mixing angles, Dirac–Fock integral ratios, and measured lifetimes.*

Spectrum	θ_2(°)	θ_0(°)	θ_1(°)	R_{31}/R_{11}[a]	τ(ns)
Pb I	39.82[b]	−22.16[b]	32.18[b]	1.4590	5.85 ± 0.20[e]
Bi II	42.84[d]	−24.16[d]	33.15[e]	1.4224	1.56 ± 0.15[f]

[a] MCDF, this work.
[b] Energy levels from Wood and Andrew, Ref. [18].
[c] Giers *et al.*, Ref. [23].
[d] Energy levels from Crawford and McLay, Ref. [21].
[e] Energy levels from Kolyniak *et al.* Ref. [20].
[f] Henderson *et al.*, Ref. [4].

Table II. *Pb I branching fractions and transition probability rates for the $^3P^o_1$ upper level in the $6s^26p^2$–$6s^26p7s$ multiplet*

Transition	λ(Å)[a]	BF(N)[b]	BF(R)[c]	BF(M)[d]	A(ns^{-1})[e]
$^3P_0$–$^3P^o_1$	2833.89	0.489	0.310	0.324	0.0529
$^3P_1$–	3640.61	0.128	0.166	0.188	0.0284
$^3P_2$–	4058.95	0.381	0.520	0.500	0.0889
$^1D_2$–	7230.96	0.0029	0.0040	0.0005	0.00068
$^1S_0$–	17181	7×10^{-5}	3×10^{-5}	—	6×10^{-6}

[a] Vacuum wavelengths.
[b] Nonrelativistic, $R_{13}/R_{11} = 1$.
[c] Relativistic, $R_{13}/R_{11} = 1.4590$.
[d] Measured, Ref. [22].
[e] Relativistic, using BF(R) and $\tau = 5.84$ ns.

Table III. *Bi II branching fractions and transition probability rates for the $^3P^o_1$ upper level in the $6s^26p^2$–$6s^26p7s$ multiplet*

Transition	λ(Å)[a]	BF(N)[b]	BF(R)[c]	A(ns^{-1})[d]
$^3P_0$–$^3P^o_1$	1436.83[e]	0.43	0.25	0.20
$^3P_1$–	1777.11[e]	0.12	0.16	0.13
$^3P_2$–	1902.31[f]	0.44	0.59	0.47
$^1D_2$–	2804.2[e]	0.004	0.005	0.004
$^1S_0$–	3933.3[e]	0.0002	0.0009	0.0002

[a] Vacuum wavelengths.
[b] Nonrelativistic, $R_{13}/R_{11} = 1$.
[c] Relativistic, $R_{13}/R_{11} = 1.4224$.
[d] Relativistic, using BF(R) and $\tau = 1.56$ ns.
[e] Reader and Corliss, Ref. [26].
[f] Wahlgren *et al.*, Ref. [27].

the relativistic branching fractions for use with the measured lifetime for computation of transition probability rates, which are also given in Tables II and III. On the basis of the agreement between relativistic and measured branching ratios in Pb I, the transition probability rates for Bi II given in Table III are probably an improvement over the nonrelativistic values that were reported in [4].

Although spectroscopic data for the members of this sequence past Bi II are not available because of their nuclear instability, the slowly varying behaviour exhibited by the mixing angles and radial matrix ratios should permit a reliable extrapolation to these systems.

4. Conclusions

The relativistic formulation presented here provides an extension of semiempirical methods which combine measurements of the energies and lifetimes of atomic levels through intermediate coupling calculations. In appropriate cases this can improve the reliability of predictive data systematizations, and allow their application to additional systems. Although the approach used here introduces theoretical values into an otherwise fully empirical exposition, the application of the theoretically obtained correction factor is merely a mapping factor between the measured data and a linearizing exposition, and does not prejudice the predictions toward *ab initio* values. Alternatively, in systems for which lifetime measurements exist for a sufficient number of upper levels within the multiplet, R_{13}/R_{11} could be determined empirically.

The ability to obtain branching fraction estimates by these methods is of importance, since almost no reliable branching fraction information is available for ions [25], and these quantities are necessary for the determination of transition probability rates and oscillator strengths from lifetime measurements.

Acknowledgement

The work was supported by the US Department of Energy, Office of Basic Energy Sciences, Division of Chemical Sciences, under Grant number DE-FG02-94ER14461.

References

1. Curtis, L. J., Phys. Rev. **A40**, 6958 (1989).
2. Curtis, L. J., Physica Scripta **43**, 137 (1991).
3. Curtis, L. J. and Ellis, D. G., J. Phys. **B29**, 645 (1996).
4. Henderson, M., Curtis, L. J., Ellis, D. G., Irving, R. E. and Wahlgren, G. M., Astrophys. J. **473**, 565 (1996).
5. Edlén, B., Physica Scripta **17**, 565 (1978).
6. Träbert, E. and Curtis, L. J., Physica Scripta **48**, 586 (1993).
7. Curtis, L., J. Phys. **B26**, L589 (1993).
8. Curtis, L. J. *et al.*, Phys. Rev. **A51**, 4575 (1995).
9. Cohen M. and Dalgarno, A., Proc. Roy. Soc. **A275**, 492 (1963).
10. Laughlin, C. and Dalgarno, A., Phys. Lett. **A35**, 61 (1971), and references cited therein.
11. Curtis, L. J., Rudzikas Z. B. and Ellis, D. G., Phys. Rev. **A44**, 776 (1991).
12. Lawrence, G. M., Astrophys. J. **148**, 261 (1967).
13. Garstang, R. H., J. Res. Nat. Bur. Std. Sect. **A68**, 61 (1964).
14. Kwela, J., Zachara, S. and Hults, M., J. Opt. Soc. Am. **73**, 1074 (1983).
15. Curtis, L. J., Ellis, D. G. and Martinson, I., Phys. Rev. **A51**, 251 (1995).
16. Bethe H. A. and Salpeter, E. E., "Quantum Mechanics of One-and Two-Electron Atoms," (Springer, Berlin 1957), p. 87.
17. Dyall, K. G., Grant, I. P., Johnson, C. T., Parpia, F. A. and Plummer, E. P., Comp. Phys. Commun. **55**, 425 (1989); Parpia, F. A., Fischer, C. F. and Grant, I. P., Comp. Phys. Commun. **94**, 249 (1996).
18. Wood, D. R. and Andrew, K. L., J. Opt. Soc. Am. **58**, 818 (1968).
19. Wood, D. R., Andrew, K. L., Giacchetti, A. and Cowan, R. D., J. Opt. Soc. Am. **58**, 830 (1968).
20. Kolyniak, W., Kornalewsky, T. and Roszkowska, K., Acta. Phys. Pol. **A49**, 679 (1976).
21. Crawford, M. F. and McLay, A. B., Proc. Roy. Soc. (London) **143**, 540 (1934).
22. Lotrian, J., Guern, Y., Cariou, J. and Johannin-Gilles, A., J. Quant. Spectrosc. Radiat. Transfer **21**, 143 (1979).
23. Giers, D. H., Atkinson, J. B. and Krause, L., Can. J. Phys. **62**, 1616 (1984), and other measurements cited therein.
24. Curtis, L. J. and Ellis, D. G., J. Phys. **B11**, 543 (1978).
25. Curtis, L. J., "Precision Oscillator Strengths and Lifetime Measurements," "Atomic Molecular and Optical Physics Handbook," (Edited by G. W. F. Drake) (AIP Press 1996), pp. 206–12.
26. Reader, J. and Corliss, C. W., "Wavelengths and Transition Probabilities for Atoms and Atomic Ions, Part I – Wavelengths," Nat. Stand. Ref. Data Ser. 68, (1980).
27. Wahlgren, G. M. *et al.*, Astrophys. J. **435**, L67 (1994).